Leal A. Hamza
Sameer H. Al-nesrawy

Department of Physics,
College of Education for Pure Sciences,
University of Babylon,
Hilla, 51001, IRAQ

Influence of Ferrite Nanoparticles Addition on Structural and Dielectric Properties of PS/PMMA Blend for Gamma Shielding Application

This study aims to synthesize a new type of nanocomposites based on polystyrene (PS)-poly(methyl methacrylate) (PMMA) blended with ferrite ($ZnNiFe_2O_4$) nanoparticles using a casting method. The results showed that the FE-SEM analysis confirmed that the (ferrite) nanoparticles have a homogeneous distribution in the PS/PMMA matrix. The dielectric properties showed that at lower frequencies, the dielectric constant (ε') shows high values; as the frequency increases, the values of (ε') decrease. At low applied frequencies, the dielectric loss (ε″) values are high; however, as the frequency increases, they decrease. The A.C. electrical conductivity ($\sigma_{A.C.}$) of nanocomposites increases with increasing frequency. As the concentration of ferrite nanoparticles increases, so do the dielectric constant, dielectric loss, and A.C. electrical conductivity. Good linear attenuation coefficients for gamma radiation are found in films with varying weight percentages of ferrite and PS-PMMA blends.

Keywords: Dielectric properties; Gamma shielding; Polystyrene; Ferrites
Received: 5 April 2025; **Revised:** 4 June 2025; **Accepted:** 11 June 2025

1. Introduction

New delivery systems have been created as a result of developments in polymer science. New polymers have been introduced, leading to the creation of polymers with special characteristics [1]. Polymer nanocomposites come in new types of particles filled with polymers, in which dispersed particles range in size from nanometers to micrometers. Materials of the nanocomposite consisting of nanoscale particles and a polymeric matrix have shown a great opportunity in the rubber industry and the thermoplastic to fabricate new products with of enhanced unique features [2]. Spinel ferrites have a closed-packed cubic structure, and researchers have widely studied them to investigate their structural, electrical, and magnetic properties [3]. Nickel ferrite is a soft magnetic material with several applications in electronic devices, such as inductors and transformer cores [4]. It is possible to modify polymer systems containing metal nanoparticles to display unique optical, magnetic, and electrical characteristics [5]. Because of its unique qualities, including its easy processing, low cost, lightweight nature, and good environmental stability, polystyrene (PS) is one of the most intriguing polymers [6]. The amorphous polymer PS has large side groups. General purpose PS is a glass-like thermoplastic that is transparent, hard, and rigid at room temperature. When heated, it can become pliable and distorted. It dissolves in cyclohexane, chlorinated hydrocarbons, and aromatic hydrocarbon solvents [7]. PMMA is one of the most well-known and oldest polymers. Because of its appealing physical and optical qualities, it is a vital and intriguing polymer with a wide range of applications [8]. PMMA is a transparent thermoplastic that is made from the MMA monomer and can be produced by bulk polymerization, emulsion, or solution. Because of its excellent optical properties and strong resistance to sunlight exposure, this acrylate is widely used to enhance and replace glass performance. This polymeric compound is stable and affordable due to its attractiveness [9].

2. Experimental Part

The PS/PMMA-$ZnNiFe_2O_4$ nanocomposites were prepared by casting method, its include dissolving of 75 wt.% of PS and 25 wt.% of PMMA in 100 mL of chloroform with a magnetic stirrer to mix the polymers for 15 minutes without temperature to obtain an additional homogeneous solution. Ferrite nanoparticles were added to the solution in varying weight percentages (1, 3, and 5 wt.%) using an ultrasonic device for five minutes and then using the casting method to fabricate PS/PMMA-$ZnNiFe_2O_4$ nanocomposites in the glass petri dish. The field-emission scanning electron microscope (FE-SEM) and dielectric properties were used to investigate the nanocomposite prepared.

3. Results and Discussion

The FE-SEM images of the PS/PMMA blend with varying $ZnNiFe_2O_4$ nanoparticle concentrations before sintering and after sintering at 1100°C are displayed in Fig. (1). The pure blend's FE-SEM image (Fig. 1a) displays a homogeneous morphology. The surface morphology of the blend is significantly altered into a uniform morphology with spherically shaped nanoparticles following the addition of 1, 3, and 5 wt.% ferrite nanoparticles (Fig. 1b, c, d, e, f, and g, respectively). The surface morphology of the PS-PMMA/ferrite nanocomposites is clearly in the films, displaying numerous aggregates, agglomerations, or randomly distributed chunks of nanoparticles [8]. Nanoparticles made of ferrite before sintering at weight 1 wt.% have an average diameter of 77.986 nm, at weight 3 wt.% have an average diameter of 35.26 nm, and at weight 5 wt.% have an average diameter of 16.308 nm. Whereas those made of Zn Ni Fe_2O_4 at sintering 1100°C at weight of 1 wt.% have an average diameter of 24.187 nm, at weight 3 wt.% have an average diameter of 14.083 nm, and at weight 5 wt.% have an average diameter of 32.841 nm.

The A.C electrical properties of the PS/PMMA-$ZnNiFe_2O_4$ nanocomposites were studied over frequencies ranging from 100 Hz to 5 MHz. The dielectric constant was calculated by using the following equation:

$$\varepsilon' = C_p/C_0 \quad (1)$$

Figure (2) shows how the dielectric constant (ε') of PS/PMMA-ferrite nanocomposite films varies with frequency before and after sintering at 1100°C. It can be deduced from these figures that the additions are in varying ratios (1, 3, and 5 wt.%). The dielectric constant (ε') is high at lower frequencies and noticeably decreases with increasing frequency which attributed to decrease the space charge polarization [10,11].

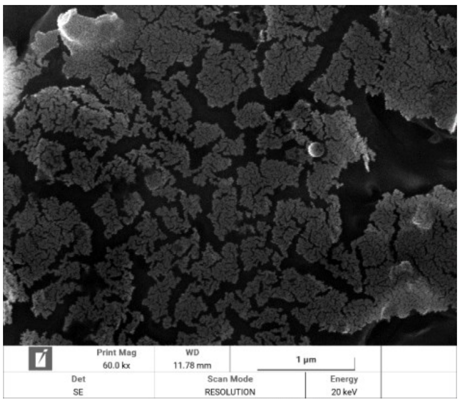

(a)

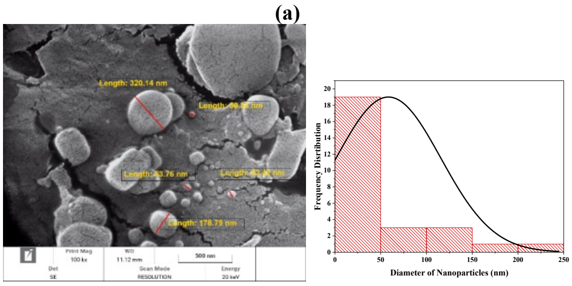

(b)

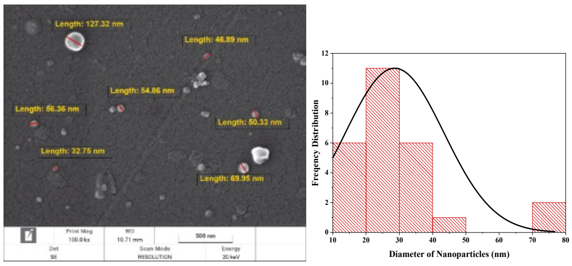

(c)

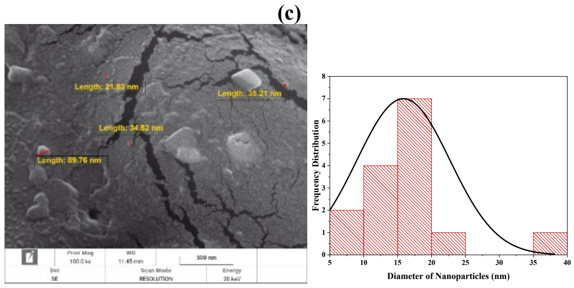

(d)

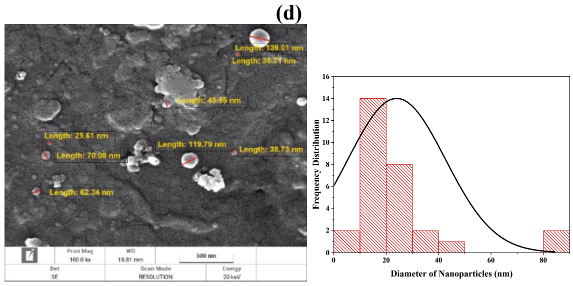

(e)

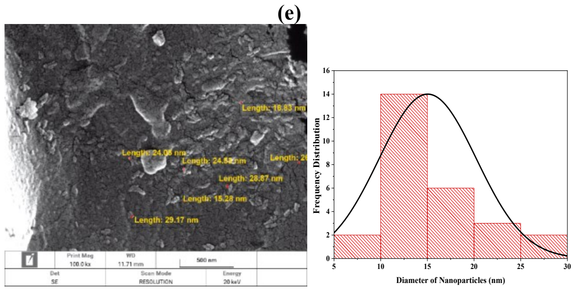

(f)

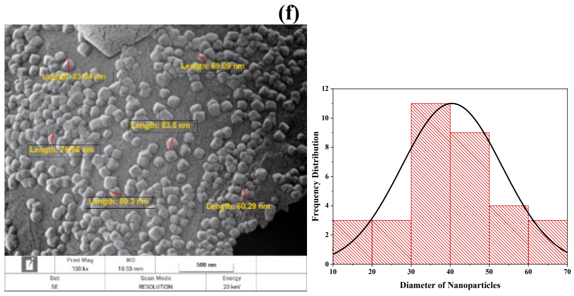

(g)

Fig. (1) FE-SEM images for PS/PMMA-$ZnNiFe_2O_4$ nanocomposites films (a) Blend PS/PMMA, (b) 1 wt.% of ferrite before sintering, (c) 3 wt.% of ferrite before sintering, (d) 5 wt.% of ferrite before sintering, (e) 1 wt.% of ferrite at sintering 1100°C, (f) 3 wt.% of ferrite at sintering 1100°C, and (g) 5 wt.% of ferrite at sintering 1100°C

The impact of adding Zn-Ni ferrite nanoparticles on the dielectric constant (ε′) at 100 Hz and 25°C for PS/PMMA-$ZnNiFe_2O_4$ nanocomposites films, respectively, before sintering and sintering at 1100°C. Figure (3) shows an increase in the dielectric constant (ε′) by increasing the ferrites content in the PS/PMMA

Vol. 21, No. 4, October-December 2025, pp. 514-519

matrix. This trend suggests an enhancement in the number of charge carriers induced by the ferrite nanoparticles [12]. Dielectric loss (ε″) could be calculated using the following expression [13]:

$$\varepsilon'' = \tan\delta\ \varepsilon' \quad (2)$$

where tan δ is the dissipation factor

For PS/PMMA-$ZnNiFe_2O_4$ nanocomposites, figure (4) illustrates the variations in dielectric loss (ε″) before and after sintering at 1100°C with frequency when the materials are stored at room temperature. As the measurement frequency increases, (ε″) decreases, as illustrated in Fig. (4). It is possible that its dipoles have enough time to align themselves with the electric field at lower frequencies, leading to high values for (ε″) at those frequencies [14].

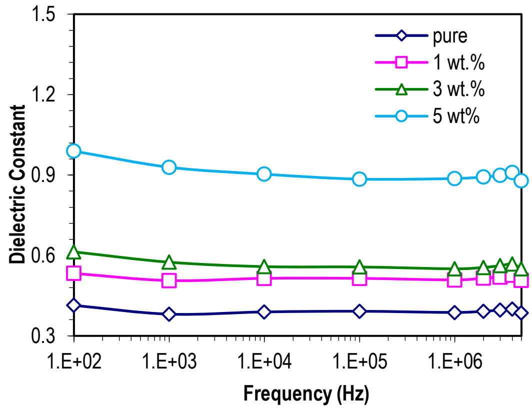

(a)

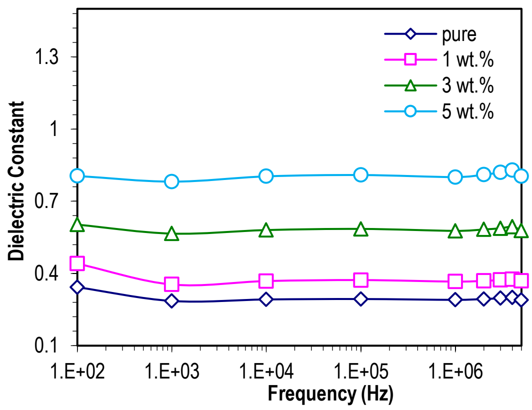

(b)

Fig. (2) Variation of dielectric constant with frequency for PS/PMMA-$ZnNiFe_2O_4$ (a) before sintering, and (b) after sintering at 1100°C

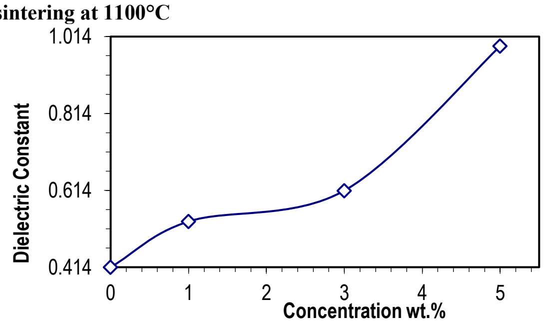

(a)

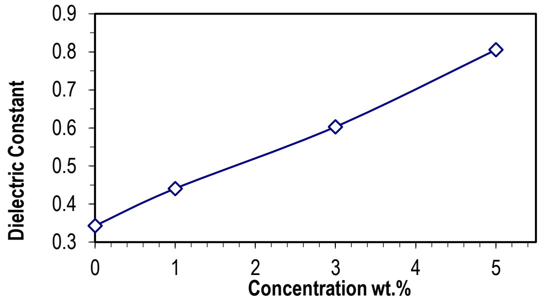

(b)

Fig. (3) Variation of dielectric constant with the ferrite concentrations for PS/PMMA-$ZnCrFe_2O_4$ (a) before sintering, and (b) after sintering at 1100°C

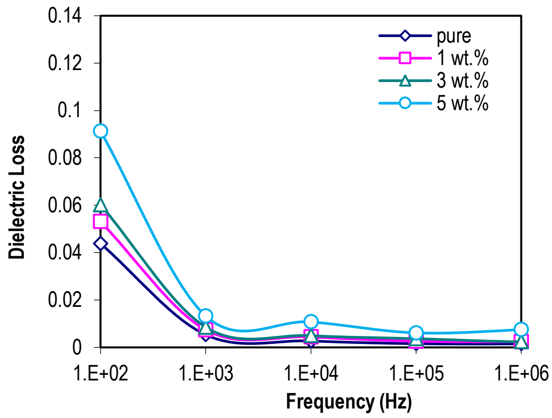

(a)

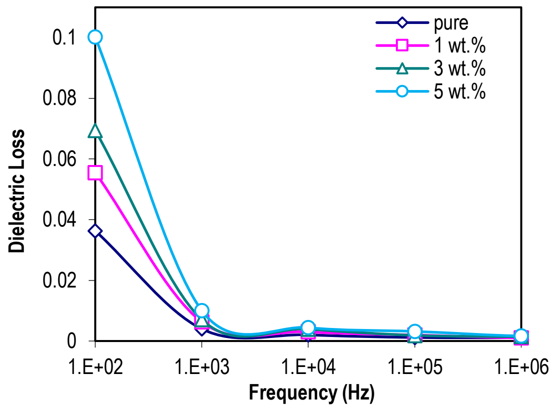

(b)

Fig. (4) Variation of dielectric loss with frequency for PS/PMMA-$ZnNiFe_2O_4$ (a) before sintering, and (b) after sintering at 1100°C

Figure (5) illustrates the relationship between dielectric loss and ferrite concentration at room temperature. It is a function of the weight percentage of ferrite nanoparticles and is caused by an increase in the number of electrons in the nanocomposites, which increases the electrical conductivity of the polymer matrix. A.C. conductivity could be found by using the following expression [15]:

$$\sigma_{A.C.} = \omega\ \varepsilon_o\ \varepsilon'' \quad (3)$$

where ω = 2πf is the angular frequency

ISSN (print) 1813-2065, (online) 2309-1673

 Vol. 21, No. 4, October-December 2025, pp. 514-519

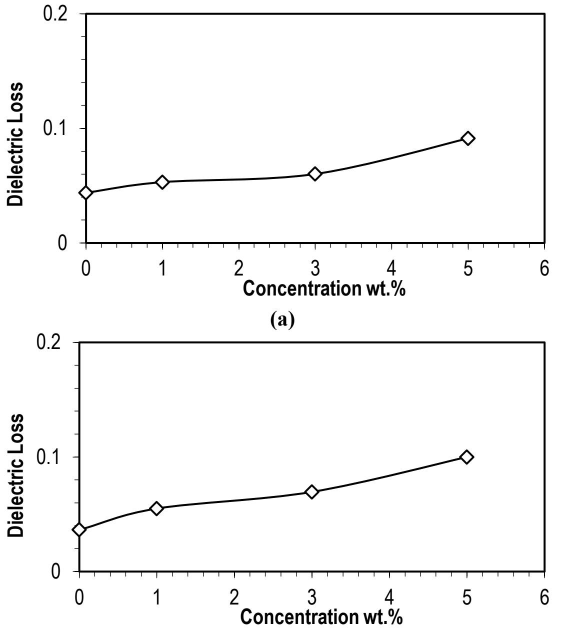

Fig. (5) Variation of dielectric loss with the ferrite concentrations for PS/PMMA-$ZnNiFe_2O_4$ (a) before sintering, and (b) after sintering at 1100°C

Figure (6) shows the variation of A.C. conductivity ($\sigma_{A.C.}$) for the applied frequency at room temperature. As the applied field's frequency rises, the A.C. conductivity progressively rises as well, especially at higher frequencies. Grain boundaries are more efficient at electrical conduction than grains at lower frequencies [16].

Because of the increase in ionic charge carriers and the formation of a continuous network of ferrite nanoparticles within the composites, figure (7) shows that the conductivity of nanocomposites has increased with increasing ferrite nanoparticle concentrations [17].

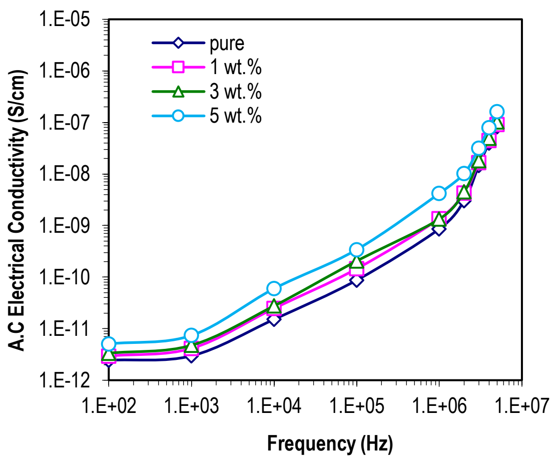

(a)

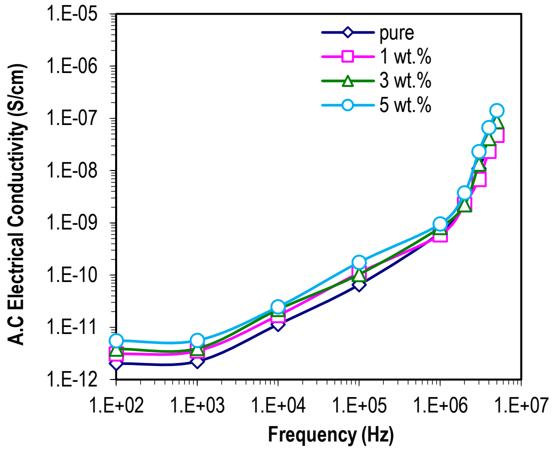

(b)

Fig. (6) Variation of the A.C electrical conductivity with frequency for PS/PMMA-$ZnNiFe_2O_4$ (a) before sintering, and (b) after sintering at 1100°C

The continuance of advances in nuclear technology led to make the radiation sources' interposition in many relevant fields such as the cultivation industry medicine nuclear power cohort and scientific research. So nuclear shields are used to decrease the exposure to nuclear radiation and their secondary interactions with the material and to reduce the effects on human tissue. Most of these shields are made from different types of materials depending on the energy type of radiation accessibility of the shielding material [18].

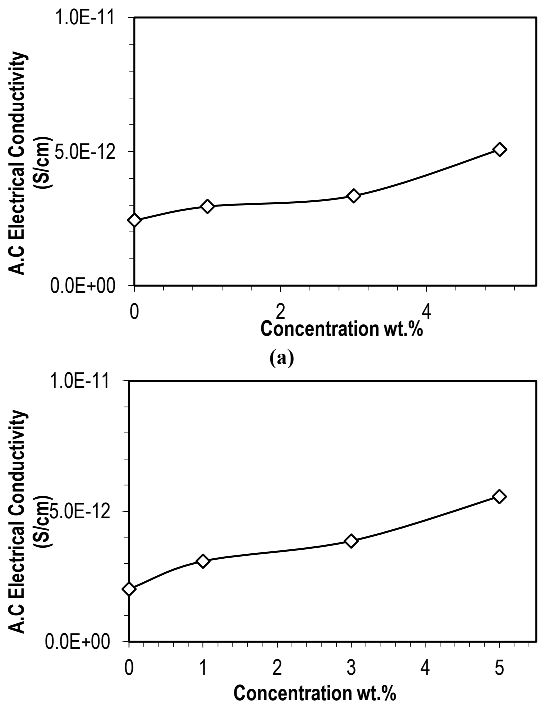

(b)

Fig. (7) Variation of the A.C. electrical conductivity with ferrite concentration for PS/PMMA-$ZnNiFe_2O_4$ (a) before sintering, and (b) after sintering at 1100°C

ISSN (print) 1813-2065, (online) 2309-1673

Polymers as matrices and fillers as reinforcements are drawing research interest in the field of radiation protection. Many published studies have attempted to develop new polymer composites as ionizing radiation shields based on high-atomic-number materials or elements other than Pb. A majority of the studies dealt with high-energy photon beams using Cs-137 gamma radiation [19]. Gamma rays are a type of electromagnetic radiation characterized by high energy levels. In contemporary times, a potential hazard exists stemming from the exposure to unshielded ionizing radiation, which arises as a consequence of the widespread application of radiation in various domains of human activity [20].

$ZnNiFe_2O_4$ nanoparticles concentrations that attributed to the increase of the attenuation radiation [22]. The range of gamma attenuation coefficients for PS-PMMA as a function of $ZnNiFe_2O_4$ nanoparticle levels is depicted in Fig. (9). The attenuation coefficient increases as the number of nanoparticles increases because the nanocomposite shielding material absorbs or reflects the gamma radiation. When comparing the obtained results by polymer nanocomposite, the figures showed very similar results. However, because of its mobility, lower electrical properties, and ability to prevent neutron emission, composite polymer has an advantage over concrete [23].

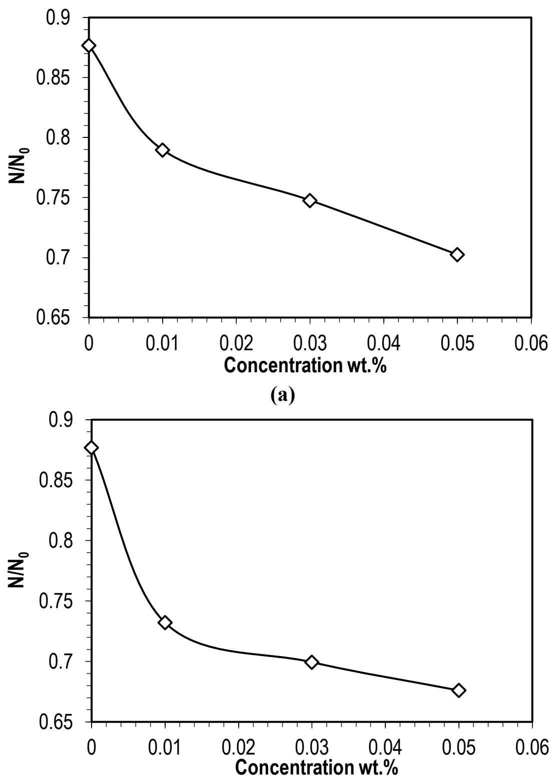

Fig. (8) Variation of N/N_0 for PS-PMMA mixture with concentration of $ZnNiFe_2O_4$ nanoparticles (a) before sintering, and (b) after sintering at 1100°C

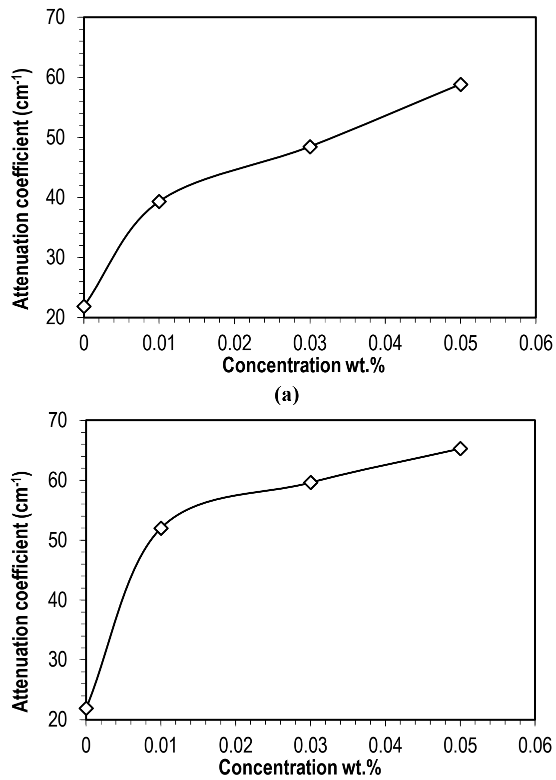

Fig. (9) Variation of gamma attenuation coefficient for PS-PMMA mixture with concentration of $ZnNiFe_2O_4$ nanoparticles (a) before sintering, and (b) after sintering at 1100°C

The equation characterizes the absorption of radiation [21]:

$$N = N_0 e^{-\mu x} \quad (4)$$

where N_0 is the number of particles of radiation counted during a certain time duration without any absorber, N is the number counted during the same time with a thickness x of absorber between the source of radiation and the detector, and μ is the attenuation coefficient is represented and measured in cm^{-1}

Figure (8) shows the variation of (N/N_0) for the PS-PMMA blend with $ZnNiFe_2O_4$ nanoparticles concentrations. As shown in the figure, the transmission radiation decreases with an increase in

4. Conclusion

The surface morphology of PS/PMMA-$ZnNiFe_2O_4$ nanocomposites shows plenty of aggregates, agglomerations, or randomly distributed chunks of nanoparticles on the film's surface. As ferrite nanoparticle concentration increases, PS/PMMA-$ZnNiFe_2O_4$ nanocomposites' dielectric constant, dielectric loss, and A.C. electrical conductivity all increase. The A.C. electrical conductivity rises with frequency, but the nanocomposites' dielectric loss and dielectric constant fall. Higher concentrations of $ZnNiFe_2O_4$ nanoparticles result in higher gamma attenuation coefficients. In an increasingly important application dimension, the prepared models demonstrated an effective ability to absorb gamma rays, enhancing their potential for use in radiation protection technologies in medical, nuclear, and military environments alike.

References

[1] M.A. Habeeb and L.A. Hamza, "Structural, Optical and D.C Electrical Properties of (PVA-PVP-Y_2O_3) Films and Their Application for Humidity Sensor", *J. Adv. Phys.*, 6(1) (2017) 1-9.
[2] L.A. Hamza et al., "The Dielectric Properties of (PVA-PVP-Y_2O_3) Nanocomposites", *AIP Conf. Proc.*, 2834 (2023) 090040.
[3] O.A. Hammadi and N.E. Naji, "Fabrication and Characterization of Polycrystalline Nickel Cobaltite Nanostructures Prepared by Plasma Sputtering as Gas Sensor", *Phot. Sen.*, 8(1) (2018) 43-47.
[4] M.A. Alsherefi, M.H. Almaamori and M.A.H. Alshimmary, "Some of Physical Properties of Nanostructured ($Mg_{1-x}Co_xFe_2O_4$) Ferrites Prepared by Sol-Gel Method", *JUBPAS*, 26(3) (2018) 125-132.
[5] O.A. Hammadi, M.K. Khalaf and F.J. Kadhim, "Fabrication of UV Photodetector from Nickel Oxide Nanoparticles Deposited on Silicon Substrate by Closed-Field Unbalanced Dual Magnetron Sputtering Techniques", *Opt. Quantum Electron.*, 47(12) (2015) 3805-3813.
[6] L.C. Costa et al., "Electrical and magnetic properties of Polystyrene doped with Iron nanoparticles", *Polym. Bull.*, 57 (2006) 881-887.
[7] N. Hayder, M.A. Habeeb and A. Hashim, "Structural, Optical and Dielectric Properties of (PS-In_2O_3/$ZnCoFe_2O_4$) Nanocomposites", *Egyptian J. Chem.*, 62 (2019) 577-592.
[8] B.A. Kazim and S.H. Al-Nesrawy, "Thickness Influence on the Optical Properties of (PMMA-PbO) Nanocomposites", *J. Nanostruct.*, 13(4) (2023) 1031-1039.
[9] M.A. Forte et al., "Is Poly (Methyl Methacrylate) (PMMA) a Suitable Substrate for ALD? A Review", *Polymers*, 13 (2021) 1346.
[10] M.T. Ramesan et al., "Nano zinc ferrite filler incorporated polyindole/poly (vinyl alcohol) blend: Preparation, characterization, and investigation of electrical properties", *Adv. Polym. Tech.*, 37(8) (2018) 3639-3649.
[11] R.G. Kadhim, "Study the Electrical and Structural Properties of (PMMA-TiO_2) Nanocomposites", *Chem. Mater. Res.*, 7(9) (2015) 37-49.
[12] M.H. Abbas et al., "Enhanced Dielectric Characteristics of Cr_2O_3 Nanoparticles Doped PVA/PEG for Electrical Applications", *IIETA*, 33(4) (2023) 261-266.
[13] T. Blethe and D. Bloor, **"Electrical Properties of Polymers"**, 2nd ed., Cambridge University Press (2005), Ch. 3, pp. 59-60.
[14] F.H. Oraibi et al., "(PS-PMMA-ZnO) nanocomposites fabrication and investigation their electrical properties for piezoelectric application", *E3S Web of Con.*, 583 (2024) 07010.
[15] G.G. Raju, **"Dielectrics in Electric Fields"**, 2nd ed., Taylor & Francis Group (2017), Ch. 3, pp. 85.
[16] A.M. Mohammad, S.M. Ali Ridha and T.H. Mubarak, "Dielectric Properties of Cr-Substituted Cobalt Ferrite Nanoparticles Synthesis by Citrate-Gel Auto Combustion Method", *IJAER*, 13(8) (2018) 6026-6035.
[17] M.S. Toman and S.H. Al-nesrawy, "New Fabrication (PVA-CMC-PbO) Nanocomposites Structural and Electrical Properties", *NeuroQuantol.*, 19 (2021) 38-46.
[18] L.A. Alasadi and E.F. Salman, "Radioactivity: Shielding materials A review", *Int. J. Adv. Multidisc. Res. Stud.*, 3(4) (2023) 1-9.
[19] M. Almurayshid et al., "Feasibility of polymer-based composite materials as radiation shield", *Radiat. Phys. Chem.*, 183 (2021) 109425.
[20] D.A. Aloraini et al., "Radiation shielding capability and exposure buildup factor of cerium(IV) oxide-reinforced polyester resins", *e-Polymers*, 23 (2023) 20230128.
[21] L.M. Chaudhari and R. Nathuram, "Absorption Coefficient of Polymers (Polyvinyl Alcohol) by Using Gamma Energy of 0.39 MeV", *Bulg. J. Phys.*, 37 (2010) 232–240.
[22] A. Hashim, I.R. Agool, and K.J. Kadhim, "Novel of (polymer blend-Fe_3O_4) magnetic nanocomposites: preparation and characterization for thermal energy storage and release, gamma ray shielding, antibacterial activity and humidity sensors applications", *J. Mater. Sci.: Mater. Electron.*, 29 (2018) 10369-10394.
[23] Z.S. Jaber and M.A. Habeeb, "Structural and Dielectrically Properties of (CMC-PAA-ZrC) Nano Composites for Gamma Shielding Application ", *JMERD*, 44(8) (2021) 371-377.